



## **VALIDATION OF HYSTERESIS MODEL OF DEFORMATION-HISTORY INTEGRAL TYPE FOR HIGH DAMPING RUBBER BEARINGS**

N. Masaki<sup>(1)</sup>, T. Mori<sup>(2)</sup>, N. Murota<sup>(3)</sup>, K. Kasai<sup>(4)</sup>

<sup>(1)</sup> Dr. Eng., Infrastructure Products Development Department, Bridgestone Corporation, nobuo.masaki@bridgestone.com

<sup>(2)</sup> Dr. Sci., Infrastructure Products Development Department, Bridgestone Corporation, takahiro.mori1@bridgestone.com

<sup>(3)</sup> Ph. D., Infrastructure Products Development Department, Bridgestone Corporation, nobuo.murota@bridgestone.com

<sup>(4)</sup> Prof., Structural Research Center, Tokyo Institute of Technology, kasai@titech.ac

### **Abstract**

A hysteresis model for seismic response analysis called “deformation history integral type model (DHI model) has been proposed for reproducing hysteresis of high damping rubber bearing by some of the authors. But formula of this model was complex and required many parameters. Therefore the model has been improved for simplicity. The improved model is very simple because only 3 parameters are required in the model. Furthermore no switching condition in the algorithm, so the calculation can be executed straightforward. But this model well describes the hysteresis characteristics of horizontal deformation of isolators including natural rubber bearings (NR), high damping rubber bearings (HRB), and so on. In this paper, we show applicability of the DHI model for high damping rubber bearing of various sizes. This model well describes the experimental behavior of isolators including two-directional loading as well as one-directional loading at the wide range of shear strain. This model can well reproduce the horizontal restoring force for random loading including two-directional loading as well. In addition, we show flexibility of DHI model by applying various types of high damping rubber bearings.

*Keywords: High damping rubber bearings, Hysteresis model, Time history response analysis*



## 1. Introduction

Seismic isolation has gained popularity as one of countermeasures for seismic protection of structures in these decades [1]. The seismic isolation is an aseismic design concept to reduce the seismic force transmitted to the structure by supporting it with a flexible element - elastomeric isolators - at the base or sometimes middle story of the buildings, to elongate the natural period of the structure and thereby decouples it from the ground. Basically, seismic isolation systems provide functions of restoring force and energy dissipation. The elastomeric isolator, made up with layers of alternating rubber and steel plates is the most popular device for providing restoring force and damping characteristics.

Generally, seismic response analysis of seismically isolated buildings are conducted by time history analysis, and the restoring force characteristics of isolation bearings are simplified as an analytical model which consists of shear springs with non-linear hysteretic characteristics, without any consideration for geometric configuration. In previous studies, many analytical models of HRB, such as either normal or modified two-directional model which takes shear strain dependency into account, Ramberg-Osgood model or Kikuchi-Aiken model [2], have been proposed. These models express properties of HRB under one-directional horizontal loading. As examples of analytical models which express properties of HRB under two-directional shear loading, Yamamoto model [3], Wen model [4], Abe model [5, 6] or Grant model [7] are given.

In the past, new hysteresis model called “deformation history integral type model (DHI model)” was proposed by some of the authors [8]. There are mainly four merits of using DHI model. First, DHI model originally developed for finite element analysis (FEA) model, so same values of parameters can be used for FEA model and hysteresis model. Second, DHI model well describe the behavior of isolators including two-directional loading at the wide range of shear strain. Third, DHI model seems complex at first glance, however, calculation algorithm of DHI model is much simple because calculation algorithm of DHI model has no branch and if-statement is not needed in calculation program. Forth, DHI model can describe the hysteresis loop of HDR with only three material parameters.

Construction of this paper is as follows; First, background of development of DHI model and outline of DHI model are shown. Second, computing algorithm of DHI model is shown so that structural engineer can easily perform time history analysis using DHI model. Third, we clarify the physical meanings of DHI model. Fourth, we show applicability of the DHI model for high damping rubber bearing of various sizes. In addition, we show flexibility of DHI model by applying various types of HRBs. Finally, example of time history analysis using DHI model is shown.

## 2. Background of Development of DHI model

In this section, we show background of development of DHI model. First motivation was that accurate material model which can trace two-dimensional loading test of HRB as well as one-dimensional loading was needed. Furthermore, it is desirable that the same parameter values can be used for FEA model and hysteresis model of HRB for seismic response analysis. Motivated by the need, firstly we searched material model proposed in the past which can accurately trace the behaviors for two-dimensional loading test, and it was found that Simo’s viscoelasticity model can trace the two-dimensional loading test for wide range of shear strain. Since Simo’s model is material model for FEA, the model define the relation between rank-3 stress tensor and rank-3 strain tensor. Therefore the model has six degrees of freedom. Simo’s model, however, can describe the behaviors of HRB under limited loading rate only. Because loading rate dependence of Simo’s model is larger than that of real isolator. For these reasons, hysteresis characteristic of HRB ordinary is modeled by not viscoelastic model but elastic-plastic model such as bilinear model [8]. Therefore we developed new model by replacing time in Simo’s viscoelasticity model with accumulated value of shear strain increment  $\Gamma$ . The model is just DHI model. We have checked the validity of DHI model for seismic response analysis of base isolated building, and it is found that the model well describes the behavior of isolators including two-directional loading as well as one-directional loading at the wide range of shear strain.



Parallel, we check whether the model can be adoptive to hysteresis model of HRB. First, we derive the two-dimensional hysteresis model by reducing six degrees of freedom to two degrees of freedom under the assumption that horizontal deformation of laminated rubber bearings behave as simple shear. We have checked the validity of DHI model for hysteresis model as well in the privious paper [9].

DHI model does not exhibit velocity dependece, however, real rubber material has velocity dependence more or less.

### 3. Outline of DHI model

Simo's viscoelastic model is shown in Eq. (1). The model is consisted of three components.

$$S = 2 \frac{\partial W_{vol}}{\partial C} + 2 \frac{\partial \bar{W}_{dev}}{\partial C} + 2 \sum_{n=1}^N g_n \int_0^t \frac{d}{dt'} \left( \frac{\partial \bar{W}_o}{\partial C} \right) e^{-(t-t')/\tau_n} dt' \quad (1)$$

Where,  $W_{vol}$  and  $\bar{W}_{dev}$  are the volumetric and deviatoric parts of elastic stored energy function.  $\bar{W}_o$  is strain energy density function for deviatoric deformation related to viscosity.  $S$  is second Piola-Kirchhoff stress,  $C$  is right Cauchy-Green tensor,  $\tau_n$  is relaxation time of  $n$ -th viscoelastic element. DHI model was derived from Simo's viscoelastic model as shown in Eq. (2) by replacing time dependence to accumulated value of equivalent strain increment  $\Gamma$  dependence. Because accumulated value of shear strain is proportional to time.

$$S = 2 \frac{\partial W_{vol}}{\partial C} + 2 \frac{\partial \bar{W}_{dev}}{\partial C} + 2 \sum_{n=1}^N g_n \int_0^L \frac{d}{d\Gamma'} \left( \frac{\partial \bar{W}_o}{\partial C} \right) e^{-(\Gamma-\Gamma')/l_n} d\Gamma' \quad (2)$$

For understanding of the meaning of the third term of Eq. (1) and Eq. (2), we rewrite this term into differential equation form. Eq. (3) is plastic term of DHI model of differential equation form, on the other hand, Eq. (4) is viscoelastic model when  $n = 1$ . Similar to viscoelastic model, in DHI model of Eq. (3) stress after step loading is relaxed by increasing accumulated value of equivalent strain increment.

$$l \frac{dS}{d\Gamma} + S = 2 \frac{\partial \bar{W}_o}{\partial C} \quad (3)$$

$$\tau \frac{dS}{dt} + S = 2 \frac{\partial \bar{W}_o}{\partial C} \quad (4)$$

Fig.1 shows a conceptual rendering of viscoelastic model and DHI model. Basic elastoplastic model cannot describe hysteretic loop of HRB, because real hysteretic loop slightly has roundness in unloading direction. But if the stress  $S$  obeys Eq.(3), the hysteretic model can be reproducing the roundness in unloading direction.

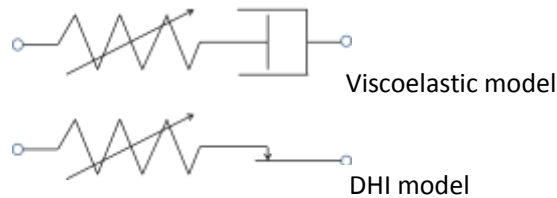


Fig.1 – Hysteretic term of viscoelastic model and DHI model

DHI model of two-dimension described by relation between shear stress and shear strain is given by



$$\begin{cases} \tau_x(\gamma_x, \gamma_y) = G_e \gamma_x \\ \quad + \sum_{i=1}^n g_i \int_0^\Gamma e^{-(\Gamma-\Gamma')/l_i} \frac{d}{d\Gamma'} \left[ \frac{1}{3} (\gamma'_x - \gamma_x) (\gamma_x'^2 + \gamma_y'^2) + \gamma'_x \right] d\Gamma' \\ \tau_y(\gamma_x, \gamma_y) = G_e \gamma_y \\ \quad + \sum_{i=1}^n g_i \int_0^\Gamma e^{-(\Gamma-\Gamma')/l_i} \frac{d}{d\Gamma'} \left[ \frac{1}{3} (\gamma'_y - \gamma_y) (\gamma_x'^2 + \gamma_y'^2) + \gamma'_y \right] d\Gamma' \end{cases} \quad (5)$$

$$\Gamma = \int_C \sqrt{d\gamma_x^2 + d\gamma_y^2} \quad (6)$$

where  $G_e$ ,  $g_1, \dots, g_n$ ,  $l_1, \dots, l_n$ , and  $n$  are the model parameters. The first and second term of Eq. (5) represents the elasticity and plasticity respectively.  $G_e$  represents the spring constant of the linear spring.  $n$  is number of multiple plastic element. If number of multiple plastic element  $n$  is 1,  $g_1$  and  $l_1$  are rewritten simply  $g$  and  $l$  respectively in this paper.  $g_i$  governs the magnitude of energy dissipation and  $l_i$  represents the unloading stiffness curvature of hysteresis curve at  $i$ -th plastic element.  $\Gamma$  is defined as curvilinear integral along the deformation orbit  $C$  on  $\gamma_x$ - $\gamma_y$  plane. (e.g. In the case of 1 cycle of circle orbit with shear strain  $(\gamma_x^2 + \gamma_y^2)^{1/2} = \gamma$ ,  $\Gamma$  becomes  $2\pi\gamma$ .) We call  $\Gamma$  accumulated value of shear strain increment.

The hereditary integral in Eq. (5) needs to be discretized to numerically calculate. In order to discretize the integral, some functions  $F$  and  $G$  are defined as follows;

$$\begin{cases} F_{xi}(\gamma_x, \gamma_y) = \int_0^\Gamma e^{-(\Gamma-\Gamma')/l_i} \frac{d}{d\Gamma'} \left[ \frac{1}{3} (\gamma'_x - \gamma_x) (\gamma_x'^2 + \gamma_y'^2) + \gamma'_x \right] d\Gamma' \\ F_{yi}(\gamma_x, \gamma_y) = \int_0^\Gamma e^{-(\Gamma-\Gamma')/l_i} \frac{d}{d\Gamma'} \left[ \frac{1}{3} (\gamma'_y - \gamma_y) (\gamma_x'^2 + \gamma_y'^2) + \gamma'_y \right] d\Gamma' \end{cases} \quad (7)$$

$$G_i(\gamma_x, \gamma_y) = \int_0^\Gamma e^{-(\Gamma-\Gamma')/l_i} \frac{d}{d\Gamma'} \left( \frac{1}{2} \gamma_x'^2 + \frac{1}{2} \gamma_y'^2 \right) d\Gamma' \quad (8)$$

where  $F_{xi}(\gamma_x, \gamma_y)$  and  $F_{yi}(\gamma_x, \gamma_y)$  are the hereditary integral of  $i$ -th plastic element in Eq. (5). Values of these functions are treated as state variables in calculation program. By doing Taylor expansion of first order, discretized hereditary integral in Eq. (5) is obtained as follows;

$$\begin{cases} F_{xi}^N = F_{xi}^{N-1} \\ \quad - \frac{F_{xi}^{N-1}}{l_i} \sqrt{\Delta\gamma_x^2 + \Delta\gamma_y^2} + \left\{ \frac{1}{3} (\gamma_x^2 + \gamma_y^2) - \frac{2}{3} G_i^{N-1} + 1 \right\} \Delta\gamma_x \\ F_{yi}^N = F_{yi}^{N-1} \\ \quad - \frac{F_{yi}^{N-1}}{l_i} \sqrt{\Delta\gamma_x^2 + \Delta\gamma_y^2} + \left\{ \frac{1}{3} (\gamma_x^2 + \gamma_y^2) - \frac{2}{3} G_i^{N-1} + 1 \right\} \Delta\gamma_y \\ G_i^N = G_i^{N-1} - \frac{G_i^{N-1}}{l_i} \sqrt{\Delta\gamma_x^2 + \Delta\gamma_y^2} + \gamma_x \Delta\gamma_x + \gamma_y \Delta\gamma_y \\ \tau_x^N = G_e \gamma_x^N + \sum_{i=1}^n g_i F_{xi}^N \\ \tau_y^N = G_e \gamma_y^N + \sum_{i=1}^n g_i F_{yi}^N \end{cases} \quad (9)$$

where  $\gamma_x^N, \gamma_y^N, \tau_x^N, \tau_y^N, F_{xi}^N, F_{yi}^N$  and  $G_i^N$  denotes  $\gamma_x, \gamma_y, \tau_x, \tau_y, F_{xi}, F_{yi}$  and  $G_i$  of  $N$  step.  $\Delta\gamma_x$  and  $\Delta\gamma_y$  are defined as  $\Delta\gamma_x = \gamma_x^N - \gamma_x^{N-1}$  and  $\Delta\gamma_y = \gamma_y^N - \gamma_y^{N-1}$  respectively.





In order to clarify the physical meaning of material parameters  $G_e$ ,  $l$  and  $g$ , we show exact solution of one-directional DHI model. In the case of monotonic loading under one-directional DHI model, Eq. (5) is calculated as,

$$\tau(\gamma) = G_e \gamma + gl \left( \frac{1}{3} \gamma^2 - \frac{4}{3} l \gamma + 2l^2 + 1 \right) - gl e^{-\gamma/l} \left( 2l^2 + \frac{2}{3} l \gamma + 1 \right) \quad (12)$$

In the case of occurring unload at shear strain  $\gamma_{\max}$  from initial load, exact solution after unloading is calculated as follows:

$$\begin{aligned} \tau(\gamma) = & G_e \gamma \\ & + gl \left( -\frac{1}{3} \gamma^2 - \frac{4}{3} l \gamma - 2l^2 - 1 \right) \\ & + gl e^{(\gamma - \gamma_{\max})/l} \left[ -\frac{2}{3} l \gamma - \frac{2}{3} \gamma_{\max} \gamma + \frac{4}{3} \gamma_{\max}^2 + \frac{2}{3} l \gamma_{\max} \right. \\ & \left. + 4l^2 + 2 - e^{-\gamma_{\max}/l} \left( 2l^2 + \frac{2}{3} l \gamma_{\max} + 1 \right) \right] \end{aligned} \quad (13)$$

From Eq. (12) and (13), if loading direction of the  $\gamma$  is positive (i.e.  $d\gamma/dt > 0$ ),  $\tau_p$  asymptotically approaches a quadratic curve represented by second term in Eq. (12). On the other hand, if loading direction of the  $\gamma$  is negative (i.e.  $d\gamma/dt < 0$ ),  $\tau_p$  asymptotically approaches a quadratic curve represented by second term in Eq. (13). This asymptotic behavior does not depend on the deformation history in the past. Namely,  $\tau_p$  is always asymptotic to the second term in the Eq. (12) or (13) depending on signal of  $d\gamma/dt$ . Hence, one-directional DHI model has asymptotic curve represented by quadratic curve, and form of quadratic curve depends on material parameter  $l$  and  $g$ .

As can be seen from the Eq. (12) and (13) as well as Eq. (5) and (6),  $G_e$  represents the spring constant of the linear spring and  $lg$  represents the magnitude of energy dissipation. Hence  $g$  governs the magnitude of energy dissipation together with parameter  $l$ . Hysteresis loop of  $\tau$  is divided into elastic part  $\tau_e$  (first term in Eq. (12) and (13)) and plastic part  $\tau_p$  (second term in Eq. (12) and second and third terms in Eq. (13)). Each behavior of hysteresis curves  $\tau_e$ ,  $\tau_p$  and  $\tau = \tau_e + \tau_p$  are shown in Fig.3.

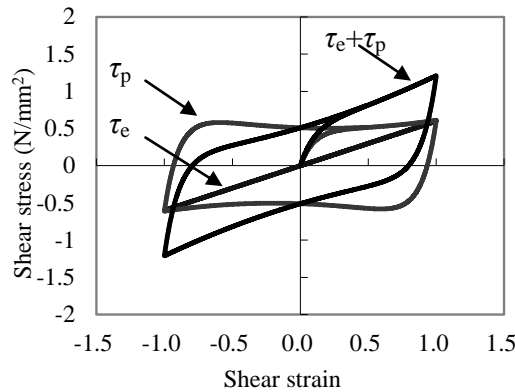


Fig. 3 – Behavior of hysteresis curve

From second term of Eq. (12) and third term of Eq. (13), shear stress approaches asymptotic curve exponentially and material parameter  $l$  characterizes the approaching rate. The smaller  $l$  is, the more instantly  $\tau_p$  approaches to asymptote. That is,  $l$  has two physical meaning. First,  $l$  governs the magnitude of energy dissipation mentioned above. Second,  $l$  characterizes the manner of curvature variations and represents the unloading stiffness curvature of hysteresis curve. Hysteresis curve behaves perfect rigid at the limit of  $l \rightarrow 0$ . Comparison between asymptotic curve and hysteresis curves with different values of  $l$  are shown in Fig.4. As



can be seen from Fig.4, if  $l$  is sufficiently small, intercept of hysteresis loop equals to  $gl(2l^2+1)$  or  $-gl(2l^2+1)$ . Summary of physical meaning of material parameters is indicated in Table 2.

Table 2 – Physical meaning of material parameters.

$G_e$	Spring constant of linear spring.
$l$	(1) Constant which characterizes the manner of curvature variations and represents the unloading stiffness curvature of hysteresis curve. (2) Constant of proportionality for magnitude of energy dissipation.
$g$	Constant of proportionality for magnitude of energy dissipation.

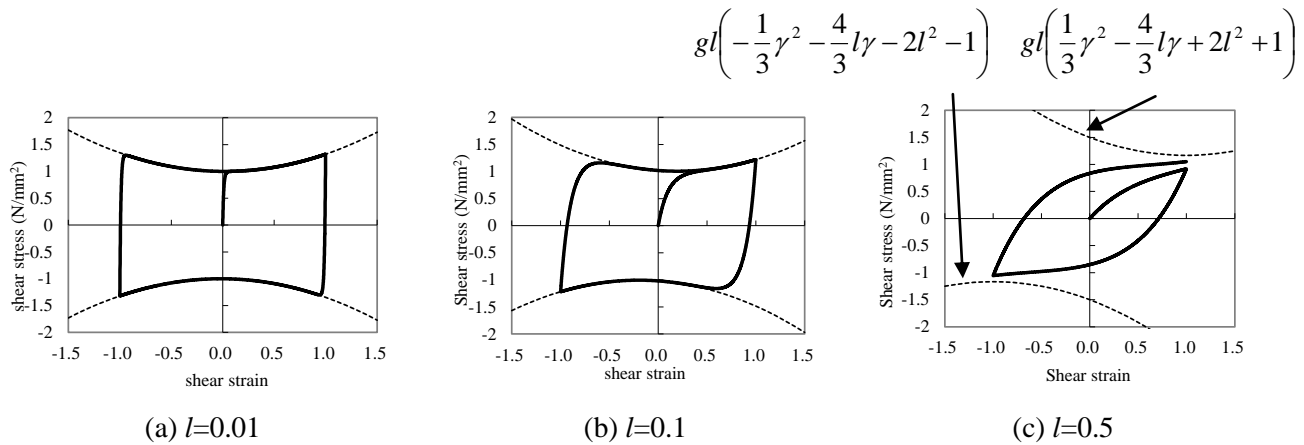


Fig. 4 – Hysteresis curves with different values of  $l$  in the case of  $gl=1$

## 5. Applicability and flexibility of DHI model

In this section, we show applicability of the DHI model for high damping rubber bearing of various sizes. In addition, we show the flexibility of DHI model by comparing analysis result with test result of two types of HRB. The one has 0.620MPa of shear modulus and 0.24 of equivalent damping ratio, the other has 0.392MPa of shear modulus and 0.22 of equivalent damping ratio. We call the former as HRB(0.6) and the latter as HRB(0.4). HRB(0.4) has smaller stiffness and smaller damping ratio compared with HRB(0.6). Material parameters for HRB(0.6) and HRB(0.4) are shown in Table 3.

Comparison of hysteresis loop between test result of HRB and analysis result is shown in Fig.5 and Fig.6. Test specimens are indicated in Table 4 and test conditions for HRB(0.6) and HRB(0.4) are shown in Table 5 and 6 respectively. As can be seen from Fig.5, analysis result shows good agreement with test result including two-directional random loading test independent of size. This applicability is one of the merits of using DHI model. In addition, as can be seen from Fig.5 and Fig.6, analysis result shows good agreement with test result independent of rubber type. So, DHI model can apply HRB independent of its stiffness or damping ratio. This flexibility is one of the merits of using DHI model as well.

Table 3 – Determination results of model parameters

	$G_e$ (N/mm <sup>2</sup> )	$g$ (N/mm <sup>2</sup> )	$l$ (-)
HRB(0.6)	0.38	0.85	0.28
HRB(0.4)	0.25	0.50	0.40





Table 4 – Test specimens

Test specimen No.	No.1	No.2-5	No.6	No.7-8
Rubber type	HRB(0.6)	HRB(0.6)	HRB(0.6)	HRB(0.4)
Outer diameter (mm)	158	225	1800	158
Inner diameter (mm)	0	0	90	0
Thickness of rubber (mm)	1.26	1.6	11.1	1.26
Number of layers	31	28	29	25
Thickness of insert plate (mm)	0.8	1.0	5.8	0.8

Table 5 – Test conditions of HRB(0.6)

Test No.	Compressive stress(N/mm <sup>2</sup> )	Wave form (Orbit) *1 *2	Test specimen No.
H6-No.1	10.7	$\gamma_{xmax}=2$ , 1cycle, $f=0.01\text{Hz}$ , $\gamma_{ymax}=1$ , 2cycle, $f=0.02\text{Hz}$ (sinusoidal)	No.1
H6-No.2	15.0	Orbit obtained from seismic response analysis result for Tokachi-Oki earthquake recorded at Hachinohe in 1968.	No.2
H6-No.3	15.0	Orbit obtained from seismic response analysis result for Tokachi-Oki earthquake recorded at Kushiro in 2003.	No.3
H6-No.4	15.0	Orbit obtained from seismic response analysis result for Tokachi-Oki earthquake recorded at Tomakomai in 2003.	No.4
H6-No.5	15.0	Orbit obtained from seismic response analysis result for Hyougo-Ken Nanbu-Oki earthquake recorded at Takatori in 1995.	No.5
H6-No.6	15.0	Orbit obtained from seismic response analysis result for Tokachi-Oki earthquake recorded at Tomakomai in 2003.	No.6
H6-No.7	15.0	Orbit obtained from seismic response analysis result for Hyougo-Ken Nanbu-Oki earthquake recorded at Takatori in 1995.	No.6

\*1 Each orbit is shown in Fig.5. \*2  $f$  represents frequency.

Table 6 – Test conditions of HRB(0.4)

Test No.	Compressive stress (N/mm <sup>2</sup> )	Wave form (Orbit) *1 *2	Test specimen No.
H4-No.1	11.0	Uni-directional loading ( $\gamma_y=0$ , sinusoidal wave) $\gamma_{xmax}=1$ (3cycle and $f=0.1\text{Hz}$ ), 2 (3cycle and $f=0.1\text{Hz}$ ), 3 (1cycle and $f=0.1\text{Hz}$ )	No.6
H4-No.2	11.0	Elliptical orbit (sinusoidal wave) $\gamma_{xmax}=1$ (3cycle and $f=0.1\text{Hz}$ ), 2 (3cycle and $f=0.1\text{Hz}$ ), 3 (1cycle and $f=0.1\text{Hz}$ ) $\gamma_{ymax}=0.5$ (3cycle and $f=0.1\text{Hz}$ ), 1 (3cycle and $f=0.1\text{Hz}$ ), 1.5 (1cycle and $f=0.1\text{Hz}$ )	No.7

\*1 Each orbit is shown in Fig.6. \*2  $f$  represents frequency.



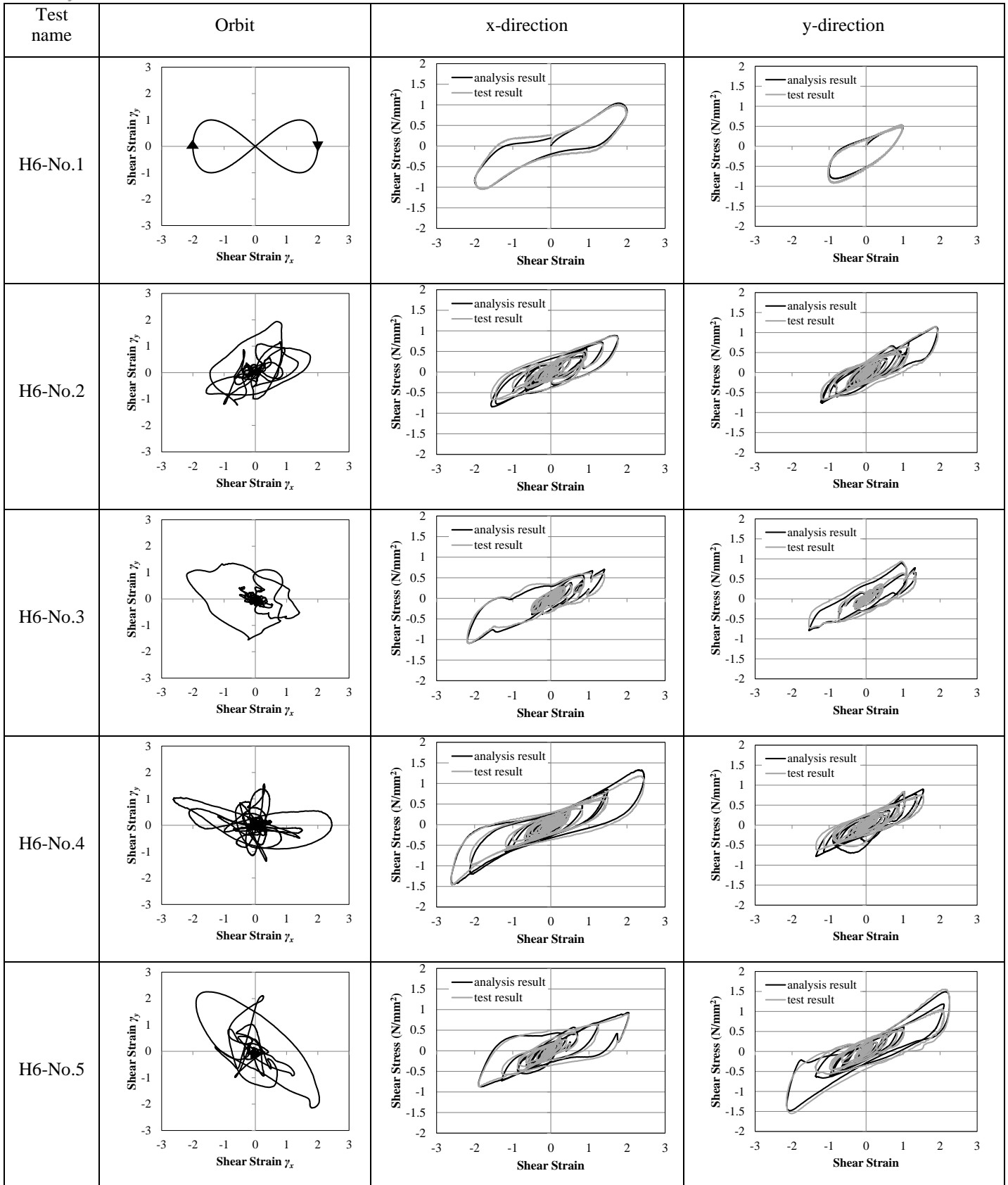


Fig. 5 – Loading orbit and comparison with test result of relation between shear stress and shear strain (HRB(0.6))

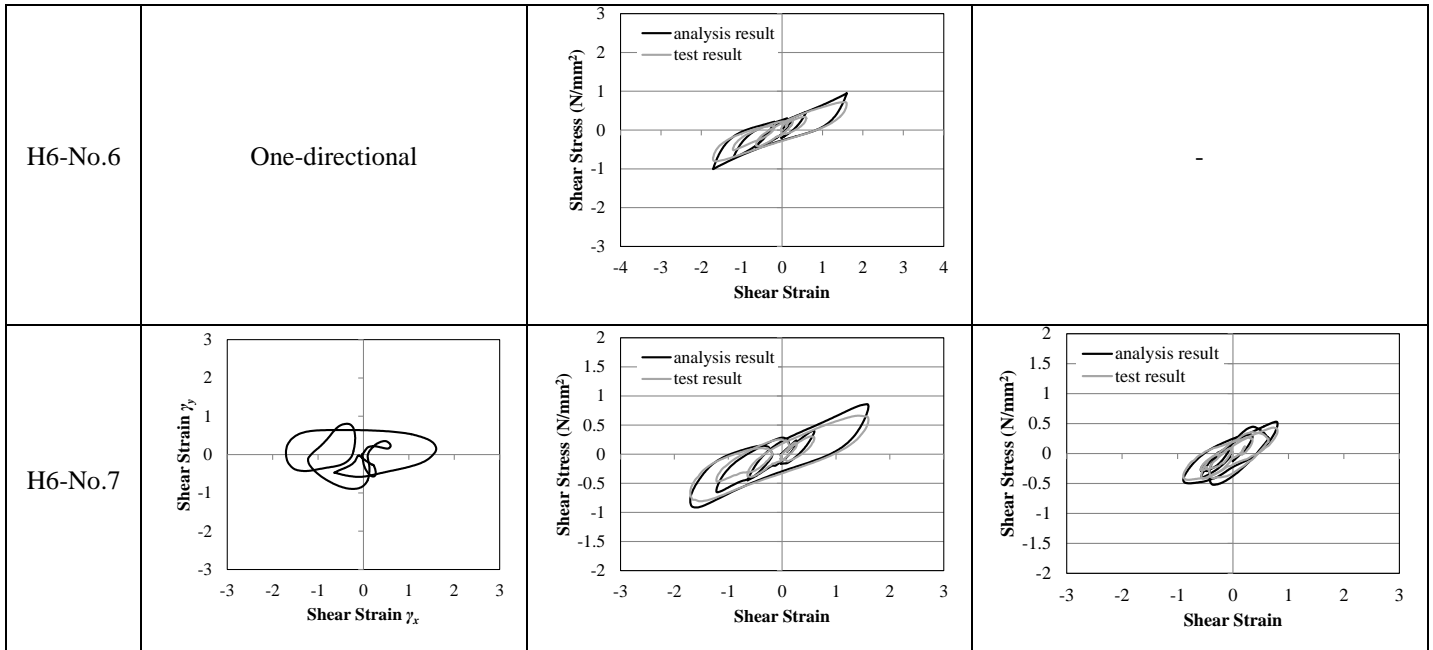


Fig. 5 – Loading orbit and comparison with test result of relation between shear stress and shear strain (HRB(0.6))

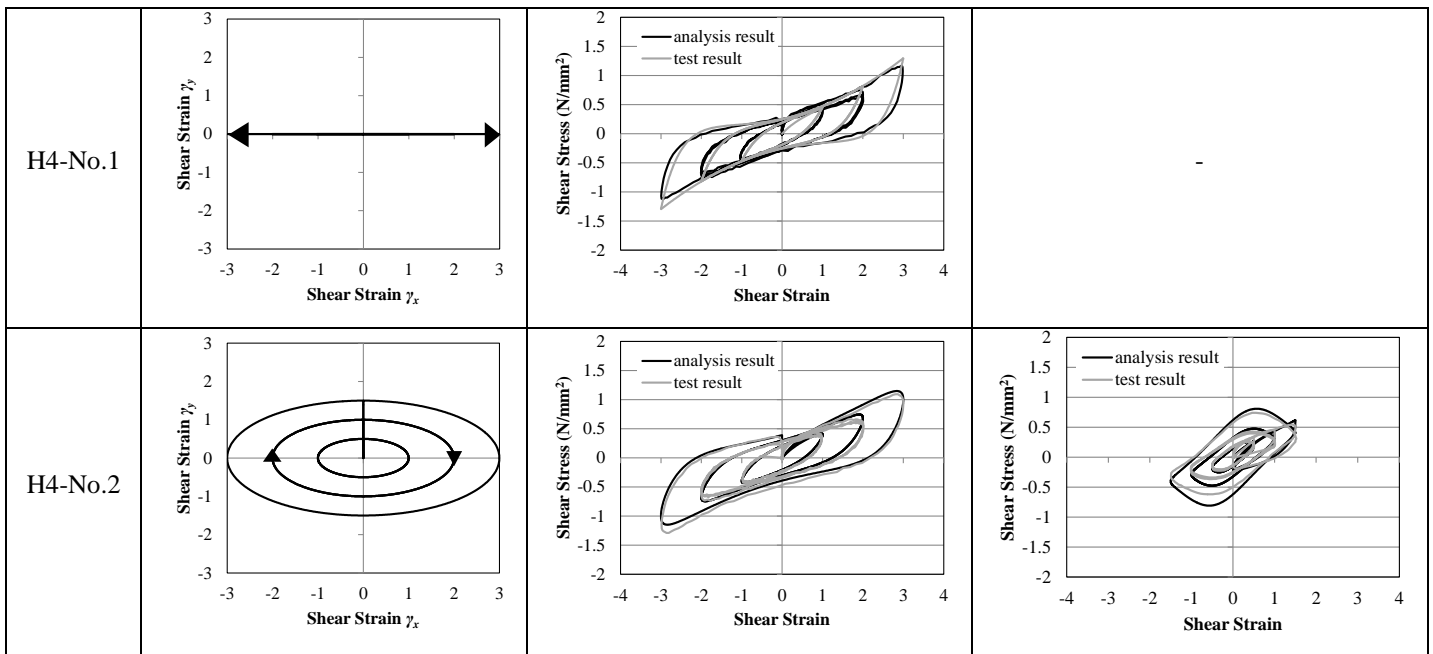


Fig. 6 – Loading orbit and comparison with test result of relation between shear stress and shear strain (HRB(0.4))

## 6. Example of time history response analysis for one mass system model

In this section, we show an example of numerical simulation. Simulation model is two-directional one mass system with high damping rubber bearing modeled by DHI model. Equation of motion is given by,



$$\begin{cases} m \frac{d^2 u_x}{dt^2} = -\tau_x (u_x / T_r) A - m \alpha_x \\ m \frac{d^2 u_y}{dt^2} = -\tau_y (u_y / T_r) A - m \alpha_y \end{cases} \quad (14)$$

where  $m$  is mass of upper structure,  $u_x$  and  $u_y$  are displacement for  $x$  and  $y$  direction respectively,  $\tau_x$  and  $\tau_y$  are shear stress of isolator for  $x$  and  $y$  direction respectively,  $A$  is effective area of isolator,  $T_r$  is total rubber thickness and  $\alpha_x$  and  $\alpha_y$  and are acceleration by earthquake for  $x$  and  $y$  direction respectively. In this example, we calculate Eq. (14) by Euler method for simplicity. Discretized Eq. (14) whose both sides divided by  $m$  for Euler method is given by,

$$\begin{cases} v_x^{N+1} - v_x^N = \Delta t \left( -\frac{\tau_x^N (u_x / T_r) A}{m} - \alpha_x^N \right) \\ v_y^{N+1} - v_y^N = \Delta t \left( -\frac{\tau_y^N (u_y / T_r) A}{m} - \alpha_y^N \right) \\ u_x^{N+1} - u_x^N = \Delta t \cdot v_x^N \\ u_y^{N+1} - u_y^N = \Delta t \cdot v_y^N \end{cases} \quad (15)$$

where  $v_x$  and  $v_y$  denote velocity for  $x$  and  $y$  direction respectively,  $\Delta t$  is time increment and  $N$  is step number of calculation. We choose high damping rubber as HRB(0.6). Earthquake acceleration and other parameters are shown in Table 7. As can be seen from Table 7, we select acceleration function as sinusoidal wave. However, frequency is different for each direction.

A result of time history analysis using HDR modeled by DHI model is shown in Fig.7. Example of program for Fortran is shown in Appendix. As can be seen from Appendix, program has no branches and so simple. This simplicity is one of the merits of using DHI model.

Table 7 – Parameter values and analysis condition

parameter	unit	value or function
$m$	kg	1500000
$A$	m <sup>2</sup>	1
$T_r$	m	0.2
$\alpha_x$	m/sec <sup>2</sup>	10 sin(2 $\pi t$ )
$\alpha_y$	m/sec <sup>2</sup>	10 sin(3 $\pi t$ )
Time increment $\Delta t$	sec	0.001
Total time	sec	10

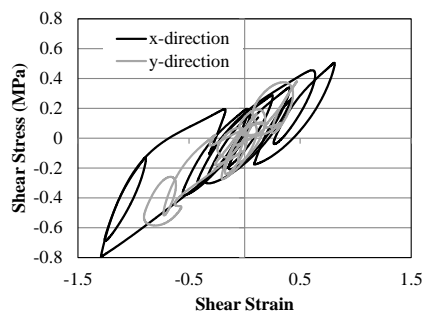


Fig. 7 – Result of time history analysis.



## 7. Conclusions

In this paper, we clarify the physical meanings show the computing algorithm of DHI model and time history analysis using the model. By comparing various test results, we show the applicability and flexibility of DHI model. In addition, we show computing algorithm of DHI model. Thus, by using DHI model, structural engineers can become designing seismically isolated structure more accurately.

## 8. References

- [1] Murota N. (2009): Earthquake Protection Materials – Reviews and Future directions of Elastomeric Isolators. *Polymers*, **58** (No.6), The Society of Polymer Science, Japan (in Japanese).
- [2] Kikuchi M, Aiken ID (1997): An analytical hysteresis model for elastomeric seismic isolation bearings. *Engng. Struct. Dyn.* **26** (2), 215-231.
- [3] Yamamoto M, Minewaki S, Yoneda H, Higashino M (2012): Nonlinear behavior of high-damping rubber bearings under horizontal bidirectional loading: full-scale tests and analytical modeling. *Earthquake Engng. Struct. Dyn.*, (Published online).
- [4] Park YJ, Wen YK, Ang AH-S(1986): Random vibration of hysteretic systems under bi-directional ground motions. *Earthquake Engng. Struct. Dyn.*, **14** (4), 543-557.
- [5] Abe M, Yoshida J, Fujino Y (2004): Multiaxial behaviors of laminated rubber bearings and their modeling. I: Experimental study. *J. Struct. Eng.* **130** (8), 1119-1132.
- [6] Abe M, Yoshida J, Fujino Y (2004): Multiaxial behaviors of laminated rubber bearings and their modeling. II: Modeling. *J. Struct. Eng.*, **130** (8), 1133-1145.
- [7] Grant DN, Fenves GL, Whittaker AS (2004): Bidirectional modeling of high-damping rubber bearings. *J. Earthquake Engng.*, **8** (1), 161-185.
- [8] Fujita T, Suzuki S, Fujita S (1990): High damping rubber bearings for seismic isolation of buildings. (1st report, Hysteretic restoring force characteristics and analytical models). *Transaction of Japan Society of Mechanical Engineer*, 56,523,658-666
- [9] Kato H, Mori T, Murota N, Suzuki S, Kikuchi M (2012): A new hysteresis model based on an integral type deformation-history for elastomeric seismic isolation bearings, 15th WCEE.

## 9. Appendix

In this appendix, an example of program of time history analysis using DHI model for Fortran is shown. In this program, SI units are used. Parameters  $m$ ,  $A$ ,  $T_r$ ,  $G_e$ ,  $g$ ,  $l$ ,  $dt$  and  $\pi$  denotes  $m$ ,  $A$ ,  $T_r$ ,  $G_e$ ,  $g$ ,  $l$ ,  $\Delta t$  and  $\pi$  respectively. Variables  $u_x$ ,  $u_y$ ,  $v_x$ ,  $v_y$ ,  $du_x$ ,  $du_y$ ,  $dv_x$ ,  $dv_y$ ,  $t$ ,  $F_{Fx}$ ,  $F_{Fy}$  and  $F_G$  denotes  $u_x$ ,  $u_y$ ,  $v_x$ ,  $v_y$ ,  $u_x^{N+1}-u_x^N$ ,  $u_y^{N+1}-u_y^N$ ,  $v_x^{N+1}-v_x^N$ ,  $v_y^{N+1}-v_y^N$ ,  $t$ ,  $F_x$ ,  $F_y$  and  $G$  respectively. This program outputs time  $t$ , displacement for  $x$ -direction  $u_x$  and displacement for  $y$ -direction  $u_y$ .

```

implicit logical (a-z)
integer i
real*8 ux,uy,vx,vy,dux,duy,dvx,dvy,dt,m,A,Tr,Ge,g,l
& F_Fx,F_Fy,F_G,pi,t
c=====Definition of Parameter=====
m=1500000.d0
A=1.d0
Tr=0.2
Ge=380000.d0
g=850000.d0
l=0.28
dt=0.001d0
pi=3.14159265d0
c=====Definition of Initial Value
ux=0.d0
uy=0.d0
vx=0.d0
vy=0.d0
F_Fx=0.d0
F_Fy=0.d0
F_G=0.d0
c=====Start of Time History Analysis by Euler Method
do i=0,10000
t=dbl(i)*dt
c=====Calculation of Incremental Displacement and Velocity Using Eq. (11)
dux=dt*vx
duy=dt*vy
dvx=dt*(-Ge*A*ux/Tr/m-g*F_Fx*A/m-2.d0*d0*dsin(2.d0*pi*t))
dvy=dt*(-Ge*A*uy/Tr/m-g*F_Fy*A/m-2.d0*d0*dsin(2.d0*pi*1.5d0*t))
c=====Update of Fx, Fy and G using (5) and (6)
F_Fx=F_Fx-F_Fx/l*dsqrt(dux*dux/Tr/Tr+duy*duy/Tr/Tr)
& +(ux*ux/Tr/Tr+uy*uy/Tr/Tr)/3.d0-2.d0*F_G/3.d0+1.d0)*dux/Tr
F_Fy=F_Fy-F_Fy/l*dsqrt(dux*dux/Tr/Tr+duy*duy/Tr/Tr)
& +(ux*ux/Tr/Tr+uy*uy/Tr/Tr)/3.d0-2.d0*F_G/3.d0+1.d0)*duy/Tr
F_G=F_G-F_G/l*dsqrt(dux*dux/Tr/Tr+duy*duy/Tr/Tr)
& +ux*dux/Tr/Tr+uy*duy/Tr/Tr
c=====Update of Displacement and Velocity
ux=ux+dux
uy=uy+duy
vx=vx+dvx
vy=vy+dvx
c=====Output of Result
write(*,*)t,ux,uy
end do
end

```